LABORATORY INVESTIGATION

USCAP
UNITED STATES AND CANADIAN
ACADEMY OF PATHOLOGY
Creating a Better Pathologist

Research Article

Alternative Tissue Fixation Protocols Dramatically Reduce the Impact of DNA Artifacts, Unraveling the Interpretation of Clinical Comprehensive Genomic Profiling

Enrico Berrino[a,b,*], Sara Erika Bellomo[b], Anita Chesta[b], Paolo Detillo[c], Alberto Bragoni[a,b], Amedeo Gagliardi[a,d], Alessio Naccarati[a,d], Matteo Cereda[d], Gianluca Witel[a,b], Anna Sapino[a,b], Benedetta Bussolati[e], Gianni Bussolati[a], Caterina Marchiò[a,b,*]

[a] Department of Medical Sciences, University of Turin, Turin, Italy; [b] Candiolo Cancer Institute, FPO-IRCCS, Candiolo, TO, Italy; [c] ADDAX Biosciences srl, Turin, Italy; [d] IIGM-Italian Institute for Genomic Medicine, c/o IRCCS, Candiolo, TO, Italy; [e] Department of Molecular Biotechnology and Health Sciences, University of Turin, Turin, Italy

ARTICLE INFO

ABSTRACT

Formalin-fixed paraffin-embedded (FFPE) samples represent the cornerstone of tissue-based analysis in precision medicine. Targeted next-generation sequencing panels are routinely used to analyze a limited number of genes to guide treatment decision-making for advanced-stage patients. The number and complexity of genetic alterations to be investigated are rapidly growing; in several instances, a comprehensive genomic profiling analysis is needed. The poor quality of genetic material extracted from FFPE samples may impact the feasibility/reliability of sequencing data. We sampled 9 colorectal cancers to allow 4 parallel fixations: (1) neutral buffered formalin (NBF), (2) acid-deprived formalin fixation (ADF), (3) precooled ADF (coldADF), and (4) glyoxal acid free (GAF). DNA extraction, fragmentation analysis, and sequencing by 2 large next-generation sequencing panels (OCAv3 and TSO500) followed. We comprehensively analyzed library and sequencing quality controls and the quality of sequencing results. Libraries from coldADF samples showed significantly longer reads than the others with both panels. ADF-derived and coldADF-derived libraries showed the lowest level of noise and the highest levels of uniformity with the OCAv3 panel, followed by GAF and NBF samples. The data uniformity was confirmed by the TSO500 results, which also highlighted the best performance in terms of the total region sequenced for the ADF and coldADF samples. NBF samples had a significantly smaller region sequenced and displayed a significantly lower number of evaluable microsatellite loci and a significant increase in single-nucleotide variations compared with other protocols. Mutational signature 1 (aging and FFPE artifact related) showed the highest (37%) and lowest (17%) values in the NBF and coldADF samples, respectively. Most of the identified genetic alterations were shared by all samples in each lesion. Five genes showed a different mutational status across samples and/or panels: 4 discordant results involved NBF samples. In conclusion, acid-deprived fixatives (GAF and ADF) guarantee the highest DNA preservation/sequencing performance, thus allowing more complex molecular profiling of tissue samples.

© 2023 THE AUTHORS. Published by Elsevier Inc. on behalf of the United States & Canadian Academy of Pathology. This is an open access article under the CC BY-NC-ND license (http://creativecommons.org/licenses/by-nc-nd/4.0/).

These authors contributed equally: Enrico Berrino and Sara Erika Bellomo.
* Corresponding authors.
    E-mail addresses: enrico.berrino@ircc.it (E. Berrino), caterina.marchio@unito.it (C. Marchiò).

ELSEVIER

Introduction

Next-generation sequencing (NGS) technology allows the detection and assessment of genetic alterations in cancer tissues, and it represents an increasingly practiced approach to meet the requirements of tailored therapies. Although DNA from fresh frozen tissues would appear to be ideally suited for this type of analysis, several reasons impose the use of DNA extracted from routine formalin-fixed paraffin-embedded (FFPE) tissue blocks.[1] Notable is the bonus of the availability of well-characterized archival material, which is collected with standard, reliable, and time-honored procedures and even stored for long times (up to several years). In addition, histologic and immunohistochemical (IHC) control allows us to select and accordingly extract the correct tumoral lesion. Finally, an FFPE tissue block is often the only material available for properly addressing therapy-related questions.

Unfortunately, the poor quality of genetic material extracted from FFPE tissue blocks may impact the feasibility and reliability of NGS data.[2-4] Among the different preanalytical steps involved in the generation of FFPE tissue blocks, the most critical step is formalin fixation. Inadequate procedures, such as delayed, insufficient, or overextended fixation or the use of acidic formalin, are known to impact the results.[5] However, even following the standard use of neutral buffered formalin (NBF), extensive DNA fragmentation and chemically induced changes often affect the results.

Formaldehyde binds to the amino groups of nucleotide bases. Deamination of cytosine can lead to misinterpretation of DNA sequences, particularly to an increased identification of cytosine (C) to thymine (T) and guanine (G) to adenine (A) (C:G > T:A). Several studies[1-4,6] have investigated the detection of artifactual mutations resulting from the deamination process, a potential cause of erroneous treatments. However, false-positive mutations remain a risk for NGS analysis of DNA extracted from FFPE tissue blocks, further enhanced by the extensive fragmentation of this material.[3]

Indeed, tissue fixation in formalin is known to produce DNA fragmentation, but the degree of fragmentation varies in different tissue blocks, and in this respect, the DNA "quality" (ie, the degree of fragmentation) heavily impacts the results of genetic analysis. Several studies[7-9] indicate that a reduced size of DNA templates decreases the success rate of amplicon-based methods and even leads to false-positive data.

The formulation of NBF consists of a solution in phosphate buffer of commercial formaldehyde, a reagent known to be rich in formic acid. The latter, once linked to sodium ions in NBF, is commonly regarded as ineffective. However, we have recently shown that removal of formic acid is responsible for a significant improvement in DNA preservation,[10] indicating a possible detrimental effect of buffered acid residues on DNA. This finding was also supported by the evidence that tissue fixation based on an acid-deprived glyoxal, which is still a dialdehyde, can be approached by maintaining the histologic and immunophenotypical features of tissues.[11] There is a gap in knowledge on the real effect of tissue fixation on sequencing results, especially when sequencing is approached by means of comprehensive genomic profiling (CGP) rather than by small targeted panels, and thus, we addressed this issue in the present study.

Materials and Methods

Cases

We sampled 9 colorectal cancer (CRC) patients with surgical resection of at least 2 cm in size to allow 4 parallel fixations (36 FFPE tissue blocks in total). We also sampled a liver hepatocellular carcinoma (aka hepatoma) that underwent thermal ablation before surgery as a control of potential "necrosis-induced" DNA degradation.

The Ethics Institutional Review Board responsible for "Biobanking and use of human tissues for experimental studies"—Department of Medical Sciences, University of Turin—approved this study. Surgical specimens were processed following the undervacuum sealing and cooling procedure.[12,13] Each of the 10 collected samples was fixed for 24 hours in parallel as follows: (1) standard formalin fixation, that is, NBF (Diapath), pH 7.2 to 7.4, which represents the fixative used in daily practice and in all the previous projects[10,11,14]; (2) acid-deprived formalin fixation (ADF) prepared by ADDAX Biosciences srl, as previously reported[10]; (3) precooled ADF (coldADF), in which the sample was immersed in precooled 4% ADF and fixed for 24 hours at 4 °C, as previously described[14]; and (4) glyoxal acid free (GAF) prepared by ADDAX Biosciences srl, as previously described[11,15] for a total of 40 samples. The features of the fixatives are reported in Table 1.

A second cohort of 9 tissues (both normal and tumoral specimens) was fixed only with GAF and with "standard glyoxal" (a solution of commercial glyoxal in 0.1 M phosphate buffer, pH 7.2) for a total of 18 tissue blocks. After fixation, the samples were routinely processed and embedded in paraffin using a HistoCore PELORIS 3 Premium Tissue Processing System (Leica Biosystems).

DNA Extraction and Quantification

Two pathologists (C.M., A.B.) evaluated the histologic and pathological features of the tissue samples. Based on the hematoxylin and eosin–stained slides, we recorded 2 parameters: (1) the percentage of tumor area (%) and (2) the total tumor area (in square millimeters). DNA was purified from five 6-μm-thick sections with a QIAamp DNA FFPE Advanced Kit (Qiagen) following the manufacturer's protocol and eluted in 40 μL of nuclease-free water. We performed both fluorometric (Qubit 3.0 Fluorometer; Thermo Fisher Scientific) and spectrophotometric (NanoDrop 1000 Spectrophotometer; Thermo Fisher Scientific) analyses. The total yield of the extraction (in nanograms) was normalized for the lesion area (in square millimeters), and nanogram per square millimeter was used as the variable to define the extraction yield. The absorbance ratio between 260 and 230 nm (R230) and 280 nm (R280) was calculated by a spectrophotometer to evaluate the extraction purity.

DNA Fragmentation Assays

As part of the preanalytical quality controls (QCs), we assessed DNA fragmentation with 2 independent methods. On the one hand, we applied the Genomic DNA ScreenTape assay on the Agilent TapeStation 4150 instrument (Agilent Technologies), allowing fragment analysis for a range between 0 and 60 bp. This method provides a discrete parameter for the DNA integrity (the DNA integrity number [DIN]) and a continuous distribution of the fragments. Continuous size distribution analysis was performed as described here (Berrino et al[10]), calculating the total area under the curve for each bin of size.

On the other hand, we applied the DEPArray FFPE QC Kit (Menarini Silicon Biosystems), as previously reported.[14] Briefly, the assay is based on 2 qPCRs encompassing the same genomic region but producing amplicons of different sizes (54 and 132 bp).

Table 1
Fixatives and protocols used in the manuscript

Fixative	Formula	Time	Temperature	Producer	Reference no.
Fixatives used for DNA preanalytics and sequencing comparison					
NBF	Neutral buffered formalin	24 h	RT	Diapath	9, 10, 13
ADF	Acid-deprived formalin	24 h	RT	ADDAX Biosciences	9
GAF	Glyoxal acid free	24 h	RT	ADDAX Biosciences	10, 14
*cold*ADF	Acid-deprived formalin	24 h	4° C	ADDAX Biosciences	13
Fixatives used only for single preanalytic comparison[a]					
BG[a]	Buffered glyoxal	24 h	RT	Sigma	—

The pH was checked and assessed as 7.2-7.4. ADF: commercial 40% formaldehyde (Sigma), deprived of acid, diluted 10% in 0.1 M phosphate buffer, pH 7.2-7.4; GAF: commercial 40% glyoxal (Sigma), deprived of acids, diluted 5% in 0.1 M phosphate buffer, pH 7.2-7.4; BG: commercial 40% glyoxal (Sigma), neutralized with NaOH, diluted 5% in 0.1 M phosphate buffer, pH 7.2-7.4.
ADF, acid-deprived formalin fixation; BG, buffered glyoxal; *cold*ADF, precooled acid-deprived formalin fixation; GAF, glyoxal acid free; NBF, neutral buffered formalin; QC, quality control; RT, room temperature.
[a] BG fixation was only applied in parallel tissue cohort for a comparative study with GAF, which evaluated the DNA preanalytic QCs.

Standard curves allow quantification of the amount of each primer, and the ratio between these amounts returns a linear QC score, ranging from 0 to ∞, where 0 represents highly fragmented DNA. The assay also represents a proof of amplifiability of the DNA sample.

Comprehensive Genomic Profiling by Amplicon-Based Targeted Sequencing

One hundred nanograms of each sample was used as input for the Oncomine Comprehensive Assay (OCAv3) targeted gene panel. This kit evaluates hot spot regions of 87 and the full coding region of 48 genes (gene for the DNA assay, 135 genes) for a total of 0.397 megabyte. The libraries were prepared using the Ion AmpliSeq Library Kit Plus (Thermo Fisher Scientific) with the standard protocol. Samples were barcoded using 40 different Ion Xpress Barcodes. The Ion Library TaqMan Quantitation Kit (Thermo Fisher Scientific) allows a sensible and specific quantification to dilute each library to 100 pM. Samples were loaded into two 550 Ion Chip GeneStudio S5 Plus Systems for sequencing (Thermo Fisher Scientific) with a minimum mean read depth of 500×. Aligned files (BAM) were processed from raw data and generated by the Ion Torrent software pipeline (Torrent Suite Software 5.12; Thermo Fisher Scientific). QCs and DNA variant calls were processed using Ion Reporter Software (version. 5.10) and analyzed as previously reported.[16]

We assessed the quality of the sequencing by analyzing the library QCs, in particular the library yield, calculated as the quantity of library obtained by the Ion Library TaqMan Quantitation Kit (Thermo Fisher Scientific), in nanometers, and the library size as the median size calculated using the DNA1000 HS of the Agilent TapeStation 4150 instrument (Agilent Technologies), in base pairs. We also assessed the sequencing QC, considering the read depth (the median value of sequencing depth, in x), the read length (the mean length of the insert size postread trimming, in base pairs), the reads on target (the percentage of the reads aligned to the targeted regions, in %), the uniformity of coverage (the percentage of the analyzed genome in which the read depth is >0.2 times the mean depth, in %), and the median absolute pairwise difference (the median of the absolute values of all such differences in $\log_2$ [read count ratio] is the measure of sequencing noise important for copy number variation analysis). Higher values = reduced quality. Finally, we also evaluated the sequencing results by generating the OncoPrint of the variants, a representation of variant calling for all somatic single-nucleotide variations (SNVs) and small indels with a variant allele frequency (VAF) ≥10%.

Comprehensive Genomic Profiling by Hybrid Capture—Based Targeted Sequencing

We performed DNA sequencing on the same samples using a second NGS targeted panel, the Illumina TruSight Oncology 500. This hybrid capture—based approach comprises the coding sequence of 523 genes, with a total panel size of 1.94 Mb and 1.2 coding regions. The size of this panel allows us to evaluate tumor mutational burden and microsatellite instability (MSI) by processing the raw data using the associated Illumina local app. Briefly, 80 ng of genomic DNA was used to generate libraries that were sequenced on the NovaSeq 6000 instrument (Illumina) to reach a minimum of 150× read depth. Data were processed as previously described.[17-19] TSO500 data also allow the prediction of mutational signatures for each type of fixation by applying the MuSiCa tool for targeted sequencing.[20]

We assessed the quality of the sequencing by analyzing the sequencing QCs, in particular the read depth (the median value of sequencing depth, in x), the read length (the mean length of the insert size postread trimming, in base pairs), the coding region sequenced (in megabytes) (the size of coding region sequenced with at least 50× of depth, in megabytes), the usable MSI sites (the number of high-quality microsatellite sites), the chimerism (the variability of the libraries on the basis of the number of amplicon families and the percentage of chimeric reads, demultiplexing the unique molecular identifier [UMI] inserted during the library preparation), the reads on target (the percentage of the reads aligned to the targeted regions, in %), and the uniformity of coverage (the percentage of the sequenced region covered at 100× and 250×, in %). Moreover, we also evaluated sequencing results by considering the Jaccard index (JI), computed as a measurement of the similarity between the nucleotide alteration and the reference sequence in all chromosome locations, as previously described.[21] We calculated the JI by comparing each fixation type based on all nucleotide variants both in germline and somatic settings. We also inferred the mutational signature profile: the mutational signatures were evaluated using the 6 substitution subtypes (C > A, C > G, C > T, T > A, T > C, and T > G) with a VAF >5% and their neighboring sequences,[22] and we also generated the OncoPrint of variants: representation of variant calling for all somatic SNVs and small indels with a VAF ≥10%.

Statistical Analysis

Statistics were performed with R software v4.03. Differences in distributions were analyzed with a paired *t* test and contingency

by Fisher exact test or χ^2 test. $P < .05$ was considered statistically significant. The JI was calculated with the proxy (version 0.4-16) package of R software.

Results

Impact of the Different Fixations on DNA Preanalytic Features

We conducted a series of tests on DNA from 9 colorectal carcinomas to compare the effect of fixation with standard NBF and 2 ADF and GAF). In addition, we tested whether ADF precooling could further ameliorate DNA preservation.

We successfully purified DNA from all tissue samples (n = 40). First, we assessed whether the different protocols could affect the yield of extraction. To reduce the impact of lesion size, we normalized the total DNA extracted for size, obtaining a value representing nanograms per square millimeter for both fluorometric and spectrophotometric assays. The median levels were comparable for all fixation types (paired t test; Supplementary Fig. S1A). In line with the DNA extraction yield, the different fixation types did not impact the R230 and R280 values (Supplementary Fig. S1B, Supplementary Table S1).

To analyze in depth the degree of DNA fragmentation, we applied 2 parallel tests. The qPCR-based assay returned a QC score that was higher for ADF, *cold*ADF, and GAF specimens than for NBF specimens and significantly higher in the comparison of ADF versus NBF and *cold*ADF versus NBF specimens (Supplementary Fig. S1C, Supplementary Table S1). The automated electrophoresis TapeStation 4150 provides both punctual (DIN) and continuous information about the fragment size distribution within the sample. *Cold*ADF showed the highest DIN values overall, although differences among the different fixatives were not statistically significant (Supplementary Fig. S1C, Supplementary Table S1).

The DIN represents a static parameter to comprehensively evaluate the composition of DNA fragments within the samples, and thus, we applied unsupervised clustering to the area under the curve of each bin size (Fig. 1). We identified 3 classes of fragmentation, mostly related to the percentage of fragments <1000 bp, with a trend of lower fragmentation from the top to the bottom of the heatmap (Fig. 1). By annotating for the fixation type, we identified a polarization of ADF and *cold*ADF in the class with lower fragmentation (red and black squares in the left annotation of Fig. 1). This was confirmed by the χ^2 test ($P = .0009$). This polarization was patient independent, with the exclusion of DNAs purified from the thermoablated hepatoma, characterized by the lowest DINs and QC scores (right annotations in Fig. 1) and
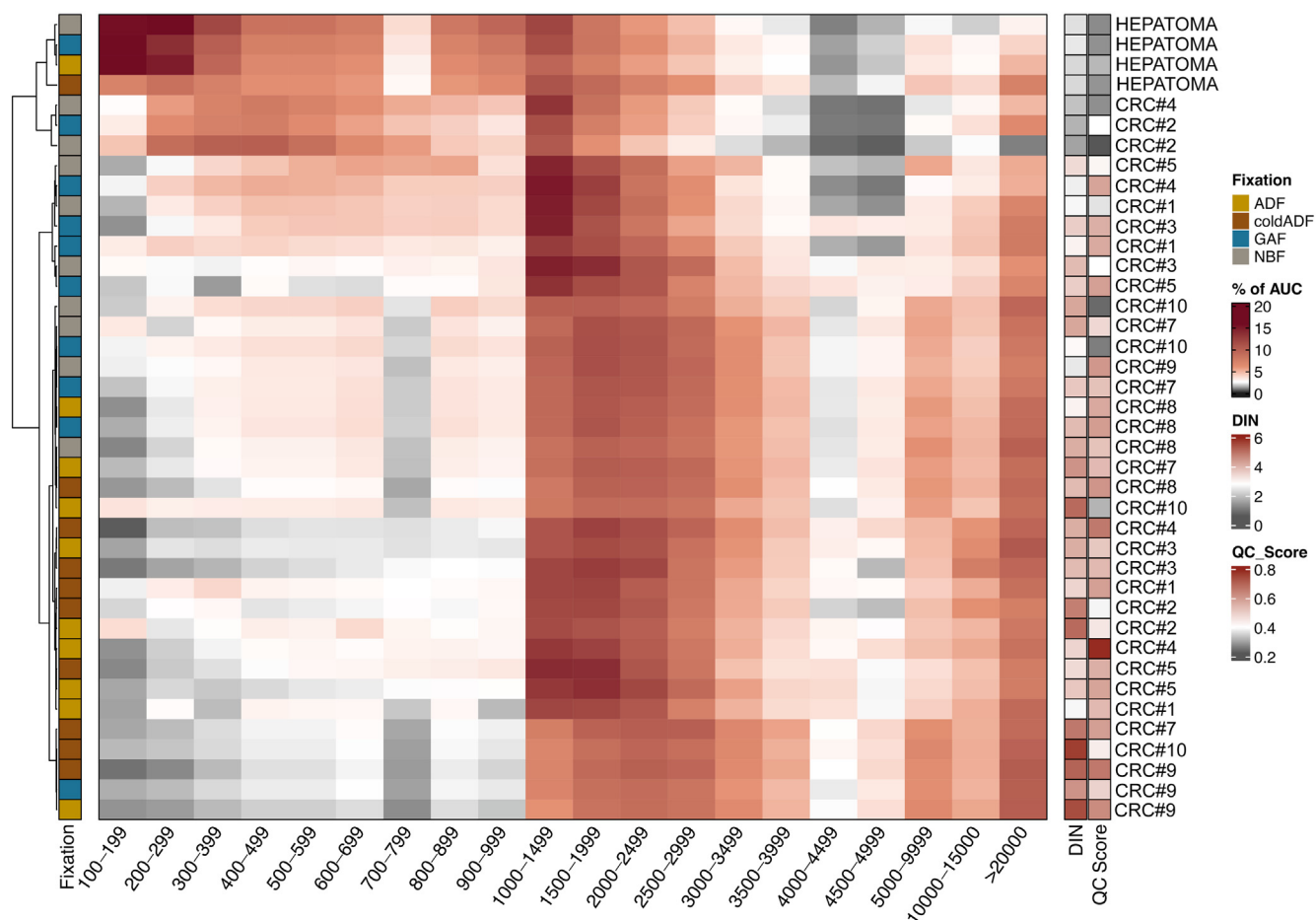

Figure 1.
Heatmap of fragmentation spectra from TapeStation data. Each row represents a single sample, with DNA size bins in columns (in base pairs). The reported parameter is the relative contribution (%) of each bin within the samples. Samples are sorted by unsupervised clustering, annotated on the left-hand side for the fixation type, and annotated on the right-hand side for the DIN and the QC score. ADF, acid-deprived formalin fixation; AUC, area under the curve; *cold*ADF, precooled acid-deprived formalin fixation; DIN, DNA integrity number; GAF, glyoxal acid free; NBF, neutral buffered formalin; QC, quality control; RT, room temperature.

clustering all together at the top of the heatmap (Fig. 1). Taken together, these results suggest an increase in terms of purity and structural integrity of the DNA after acid deprivation (from NBF to ADF/coldADF). We wondered whether this could also be applied to tissues fixed in standard buffered glyoxal versus GAF (acid-deprived glyoxal). Boxplots in Supplementary Figure S1D show a significantly higher DIN in GAF specimens than in those fixed with standard glyoxal.

Impact of the Different Fixations Over a Comprehensive Genomic Profiling Based on Amplicon-Based DNA Targeted Sequencing

Comparative results of the sequencing with the OCAv3 panel were divided into library preparation QCs, sequencing QCs, and sequencing results. In terms of library QCs, the analysis of the TapeStation electrophoresis showed a larger library size (in base pairs) for coldADF-fixed specimens, confirming the higher quality of these samples, despite a similar library yield (Supplementary Fig. S2A). Boxplots displayed comparable library sizes for GAF and ADF slightly higher than that for NBF-fixed samples.

We pooled the normalized libraries in 2 IonTorrent 550 chips to reach at least a mean depth of $500\times$. Libraries were balanced; hence, no differences in depth were identified across the different fixation types (Supplementary Table S2). After trimming, we detected a read length in line with the previous result of library size, with NBF-derived libraries being significantly shorter than the others (Fig. 2A, Supplementary Table S2). Following alignment, we calculated the fraction of reads falling on the target region together with the uniformity of spreading within that region. Despite a comparable, high level of on-target sequencing (Fig. 2B, Supplementary Table S2), uniformity was significantly reduced in NBF-fixed tissues. Conversely, ADF-derived and coldADF-derived libraries were characterized by high levels of uniformity, whereas GAF libraries were characterized by an intermediate level (Fig. 2B, Supplementary Table S2).

Amplicon-based libraries also allow the calculation of the median absolute pairwise difference, which consists of the difference between the quantity (as $\log_2$ of read count ratio) of adjacent amplicons as a measure of "amplification noise." In line with previous data, libraries from NBF tissues showed the highest level of noise significantly higher than those from ADF and coldADF (Supplementary Fig. S2B, Supplementary Table S2). Similar to previous data, libraries from GAF tissues showed a medium level of noise.

Sequencing results are reported in OncoPrint in Figure 2C. OCAV3 somatic variants are reported in Supplementary Table S3 together with the alteration identified in the TSO500 sequencing. The hepatoma did not harbor any variants in any of the parallel samples. When focusing on CRCs, we observed that CRC#9 showed more variants than the other tumor samples. At the same time, CRC#9 samples with different fixation sites harbored variability in terms of the type and quantity of detected variants. In addition, scattered and rare discrepancies were identified within parallel samples (different fixation protocols) of other CRCs (discussed below by integration of a cross-comparison with the hybrid capture−based data).

Impact of the Different Fixations Over a Comprehensive Genomic Profiling Based on a Hybrid Capture DNA Targeted Sequencing

Comparative results for sequencing with the TruSight Oncology 500 panel were divided into library sequencing QCs and

sequencing results. In line with OCAv3, median depth was not influenced by the fixation type (Supplementary Table S4), and read length comparison confirmed longer reads for ADF and coldADF, with NBF libraries being significantly shorter compared with other fixatives (Supplementary Table S4).

TSO500 is a UMI-based panel in which these short random nucleotide sequences are added to each molecule of a sample before PCR to reduce the impact of PCR duplicates. By grouping the UMI deduplicated reads into families, the pipeline returns the UMI family size (larger size → lower PCR errors) and the percentage of chimeric reads (ie, PCR duplicates). No differences were observed within the 4 fixatives for the percentage of chimeric reads; however, ADF-derived and coldADF-derived libraries showed the highest UMI family size compared with GAF and NBF (Supplementary Table S4).

The coding size of TSO500 was 1.27 Mb, and we wondered whether different fixatives could influence the total region sequenced. In line with the lower quality of the libraries, NBF showed a significantly smaller region sequenced, with both ADF-based fixatives showing the best performance (Fig. 3A, Supplementary Table S4). TSO500 also evaluates a total of 120 microsatellite loci for the MSI test. We observed a significantly lower number of evaluable microsatellite loci in NBF than in all the other fixatives (Supplementary Table S4).

The analysis of the reads on target demonstrated a significantly higher quantity of off targets in the libraries stemming from NBF-fixed samples, thus affecting the uniformity of coverage at $250\times$, which was significantly lower for NBF samples compared with the others (Fig. 3B). The OncoPrint in Figure 3C reports the 50 most frequently mutated genes with somatic variants harboring a VAF of at least 10%. The hepatoma samples were all wild type. In line with the OCAv3 results, CRC#9 showed a high mutational load (ADF = 66.3, coldADF = 76.1, GAF = 66.6, and NBF = 68.7) and a high level of MSI (ADF = 52.9%, coldADF = 48.1%, GAF = 65.7%, and NBF = 60.0%). In addition, visual inspection of OncoPrint revealed an increased number of variants for CRC#2 NBF-fixed samples only compared with the other CRC#2 samples.

Similar to the OCAv3 panel results, we observed scattered differences across the samples. To systematically evaluate similarities/discrepancies, we planned specific analyses. First, we performed cross-comparisons of somatic variants affecting the genomic regions covered by OCAv3 and TSO500 to assess the gain or loss of variants in the main cancer-related genes. Second, based on TSO500 data, we also evaluated intrapatient differences through the calculator of the Jaccard coefficient for each single base alteration (both germline and somatic with a VAF $\geq$10%, both synonymous and nonsynonymous). Finally, we assessed the variant type and predicted the mutational signature profiles.

For the cross-comparison analysis, we excluded CRC#9 because of the high number of variants and possible intrinsic heterogeneity of variants in MSI lesions. We observed a substantial overlap with 17 unique variants shared by all the samples and confirmed by both panels; however, 5 genes showed a different status across samples and/or panels (Table 2). Of these discordant results, 4 involved samples purified from NBF-fixed tissues.

CRC#3-NBF harbored a *NOTCH1* SNV (p.M1886fs) by OCAv3 sequencing, which was not identified in the other CRC#3 samples or CRC#3-NBF sequenced with the TSO500. In the same sample, the *TP53* p.R213L mutation shared by all the other lesions was not detected (by either OCAv3 or TSO500). *PIK3CA* p.H1047L was present in all CRC#4 samples by both panels, except for the OCAv3 analysis of the NBF-fixed sample.

In addition, an *ATM* variant (p.S933C) was detected only in 2/4 CRC#5 samples: both OCAv3 and TSO500 analyses did not identify
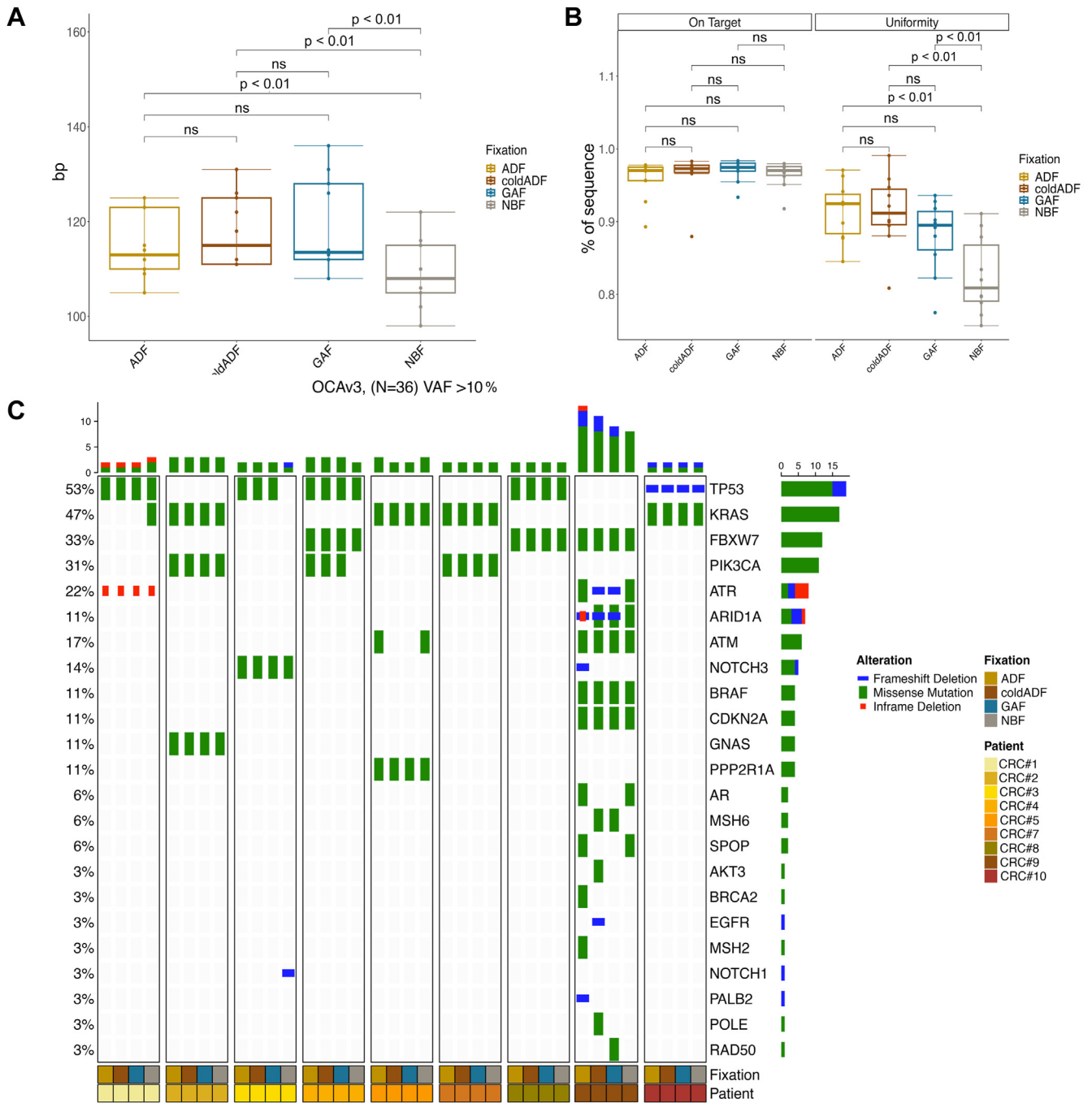
Figure 2.
Output data by the OCAV3 panel. (A) Boxplot of the OCAV3 read insert size. The *y*-axis reports the mean size for each sample grouped by the fixation protocol. The *P* value was calculated with a paired *t* test. (B) Boxplots of the percentage of on-target sequence and the uniformity of coverage. The *y*-axis reports the percentage of reads for the 2 parameters for each sample grouped by the fixation protocol. The *P* value was calculated with a paired *t* test. (C) OncoPrint of variants detected by the OCAV3 panel. Gene names and relative frequency of mutations identified in the 9 CRCs are reported on the double *y*-axis. Top annotation shows the number of variants per fixation type for each patient, whereas bottom annotations report the fixation type and the sample ID. ADF, acid-deprived formalin fixation; *cold*ADF, precooled acid-deprived formalin fixation; GAF, glyoxal acid free; NBF, neutral buffered formalin; ns, nonsignificant; VAF, variant allele frequency.

this variant in the NBF-fixed and ADF-fixed specimens. Finally, CRC#1 *cold*ADF-fixed samples showed private and subclonal *KRAS* p.G12D, which was not detected in the other samples.

TSO500 intrapanel comparison of synonymous and non-synonymous variants allowed us to calculate the JI within the fixation types, a quantitative measurement of similarity across the fixatives. By considering both germline and somatic variants, all fixations showed a high level of correlation (JI > 0.90). Of note,

ADF and *cold*ADF showed the closest similarity, whereas GAF-fixed and NBF-fixed samples showed a smaller concordance (Fig. 4A). This trend is even clearer considering only somatic variants: GAF samples showed the lowest JI compared with all the other samples (0.75 with *cold*ADF and 0.69 for both ADF and NBF), with ADF retaining a strong correlation with *cold*ADF (0.84) and NBF (0.78), in line with the JI = 0.8 between *cold*ADF and NBF (Fig. 4B).
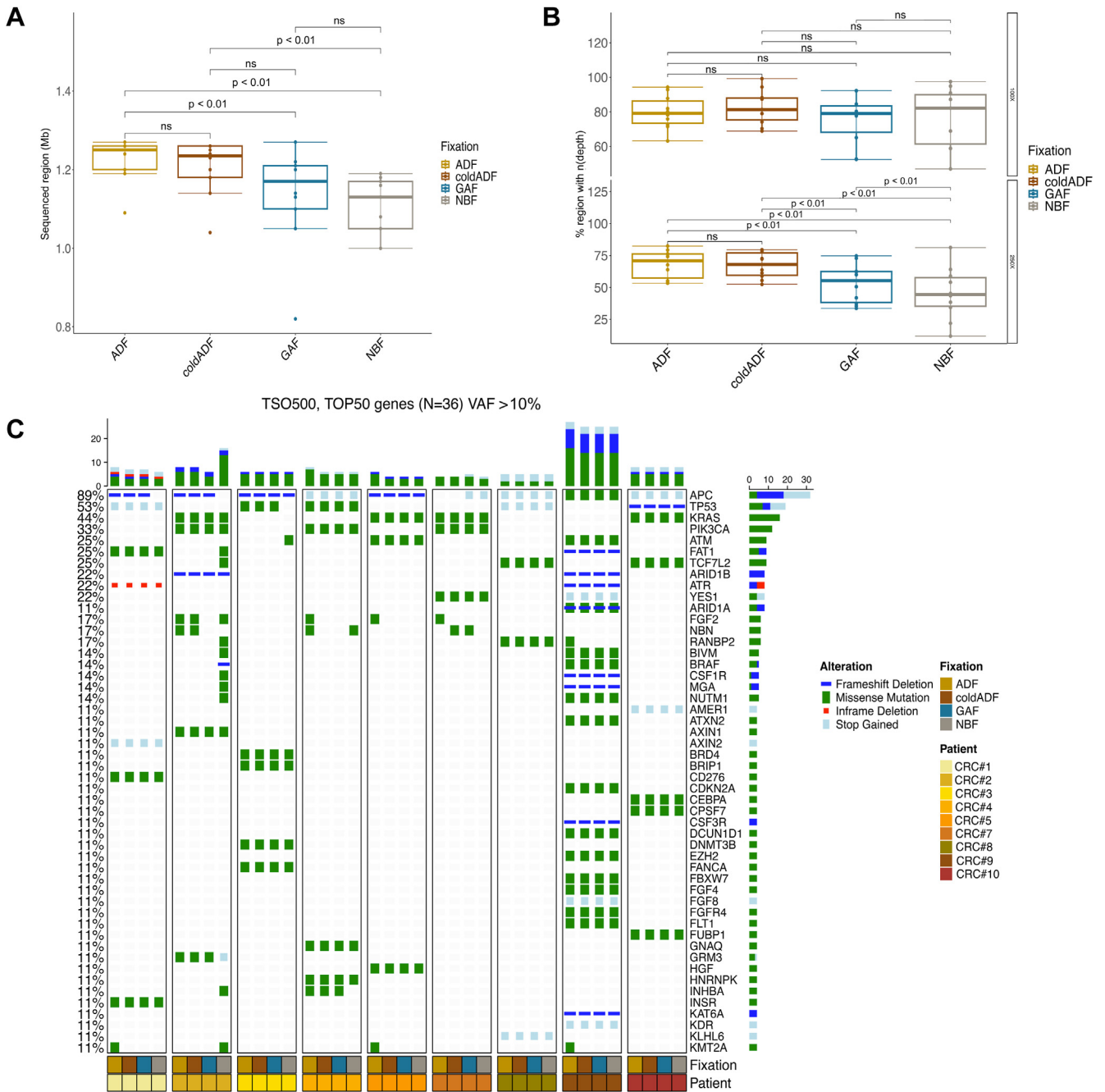
Figure 3.

Output data by the TSO500 panel. (A) Boxplot of the exonic sequenced regions. The *y*-axis reports the mean megabyte sequenced for each sample grouped by the fixation protocol. The *P* value was calculated with a paired *t* test. (B) Boxplots of the TSO500 target region sequenced at 100× and 250×. The *y*-axis reports the percentage of the target region covered at 100× and 200× for each sample grouped by the fixation protocol. The *P* value was calculated with a paired *t* test. (C) OncoPrint of the variants detected in the 50 most mutated genes. Gene names and relative frequency of mutations identified in the 9 CRCs are reported on the double *y*-axis. Top annotations show the number of variants per fixation type for each patient, whereas bottom annotations report the fixation type and the sample ID. ADF, acid-deprived formalin fixation; *cold*ADF, precooled acid-deprived formalin fixation; GAF, glyoxal acid free; NBF, neutral buffered formalin; ns, nonsignificant; VAF, variant allele frequency.

To qualitatively evaluate genetic features within the different fixations, we compared the variant type (eg, SNVs, deletions, and insertions) and the variant classification (eg, missense, synonymous, frameshift, stop-gained variant, and in-frame deletions). A significantly increased number of SNVs was present in the NBF-fixed lesions and was also associated with an increased number of missense, synonymous, frameshift, and stop-gain variants (*P* < .01 compared with all the other

fixatives; Supplementary Fig. S3A, B). No differences were identified across the other fixation protocols.

Finally, we predicted the mutational signature profiles for each fixation type. The 96-matrix profile showed similar but non-completely overlapping substitutions (Fig. 5A). By quantifying the relative contribution of each signature, we identified similar weights for signatures 6 and 15 for each fixation type related to the MSI phenotype. Signature 1, aging related but also referred to

Table 2
Sequencing discrepancy within samples and panels

ID	Gene	Variant	Fixative	OCAV3 (VAF)	TSO500 (VAF)
CRC#1	*KRAS*	p.G12D	ADF	Not identified	Not identified
			*cold*ADF	10.34	10.13
			GAF	Not identified	Not identified
			NBF	Not identified	Not identified
CRC#3	*NOTCH1*	p.M1886fs	ADF	Not identified	Not identified
			*cold*ADF	Not identified	Not identified
			GAF	Not identified	Not identified
			NBF	Not identified	13
CRC#3	*TP53*	p.R213L	ADF	19.3	17.3
			*cold*ADF	20.1	21.1
			GAF	20	16.1
			NBF	Not identified	Not identified
CRC#4	*PIK3CA*	p.H1047L	ADF	12.40	11.4
			*cold*ADF	15.10	14.5
			GAF	13.70	13.4
			NBF	Not identified	11.30
CRC#5	*ATM*	p.S993C	ADF	Not identified	Not identified
			*cold*ADF	12.3	11.2
			GAF	14.3	10.3
			NBF	Not identified	Not identified

Each row represents a patient with a sequencing incongruity. We report the affected gene, the gene variant, and the fixation type. For each panel, when identified, we reported the VAF of the alteration.

ADF, acid-deprived formalin fixation; *cold*ADF, precooled acid-deprived formalin fixation; GAF, glyoxal acid free; NBF, neutral buffered formalin; VAF, variant allele frequency.

FFPE artifacts, showed a significant reduction from NBF (37%) to ADF (30%) and GAF (31%) fixation, reaching 17% in the *cold*ADF samples (Fig. 5B).

Discussion

In this study, we report a detailed analysis on the effect of different fixation protocols on DNA integrity/preservation of tissue samples, thus providing evidence of the impact these pre-analytical features may have when performing CGP data analysis. Precision medicine in oncology is currently demanding an enormous effort in extracting the most valuable information from tissue samples.[23,24] This is particularly important for advanced-stage cancer patients. To fulfill this task, pathologists and molecular biologists use a combination of in situ techniques (IHC and in situ hybridization) and molecular profiling by in vitro nucleic acid−based assays. The latter are currently best approached by targeted NGS, with commercially available panels that can be variable in terms of size (number of genetic alterations/genes that can be analyzed). Molecular diagnostics typically use panels with a limited number of cancer-associated genes (up to 50) and a reference range that can be variable across panels. This strategy helps deconvolute the complexity of an NGS analysis on degraded DNA/RNA by focusing on a handful of targets that are specifically needed at present for treatment decision-making. Nevertheless, the number and complexity of genetic alterations to be investigated is rapidly growing (even with an agnostic manner).[25-28] In this scenario, panels limited in size may not be fit for purpose, especially when screening for molecular alterations that could be of interest for ongoing clinical trials.[25,27] Therefore, in several instances, archival FFPE tissue samples undergo a CGP analysis, which is likely to expand its applicability in the future. The challenge of a CGP approach is appreciated at 2 distinct levels: (1) the success rate of the sequencing and (2) the complexity of data interpretation. Both features largely depend on the quality of nucleic acids.

Formalin fixation has a profound effect on tissue quality, and therefore, there has been much attention to alternative fixation protocols over the years; for instance, alcohol-based non−cross-linking tissue fixatives have been proposed.[29-34] In this study, we focused on alternative aldehyde fixatives that still act by cross-linking and provide similar structural and antigenic preservation to NBF. Nevertheless, they allowed a critical improvement in DNA preservation compared with classical NBF fixation. We tested both ADF, obtained by the removal of the formic acid residues present in the commercial formaldehyde reagent via ion-exchange resins,
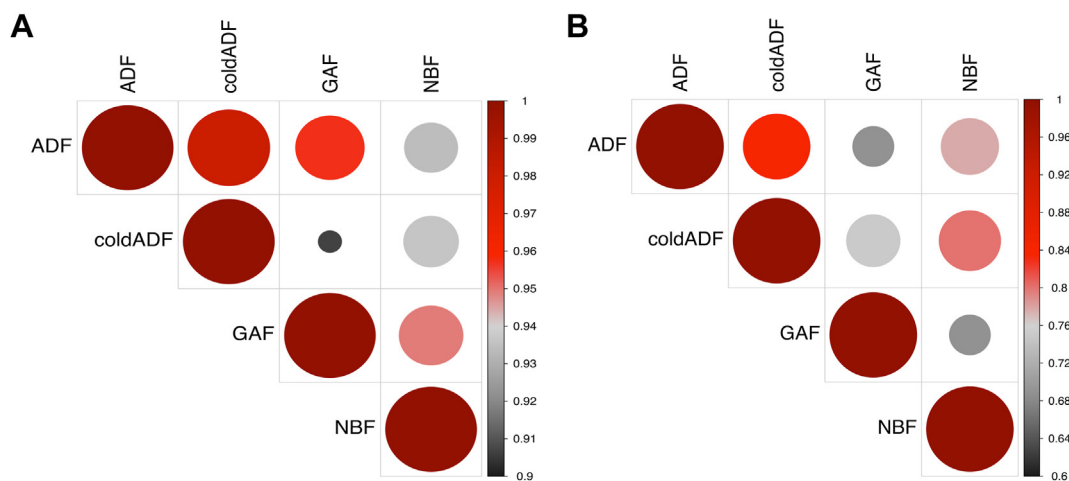

Figure 4.
Correlations across samples and gene panels. (A) Correlation plot of the JI germline variant comparison. The size and color of the bullets summarize the similarity within the fixation types. Red and larger dots are proper fixatives with similar nucleotide changes, whereas grayish and smaller bullets represent fixatives with more variable changes. The scale bar of JI for germline comparison ranges from 0.9 to 1.0. (B) Correlation plot of the JI somatic variant comparison. The size and color of the bullets summarize the similarity within the fixation types. Red and larger dots are proper fixatives with similar nucleotide changes, whereas grayish and smaller bullets represent fixatives with more variable changes. The scale bar of JI for somatic comparison ranges from 0.6 to 1.0. ADF, acid-deprived formalin fixation; GAF, glyoxal acid free; JI, Jaccard index; NBF, neutral buffered formalin.
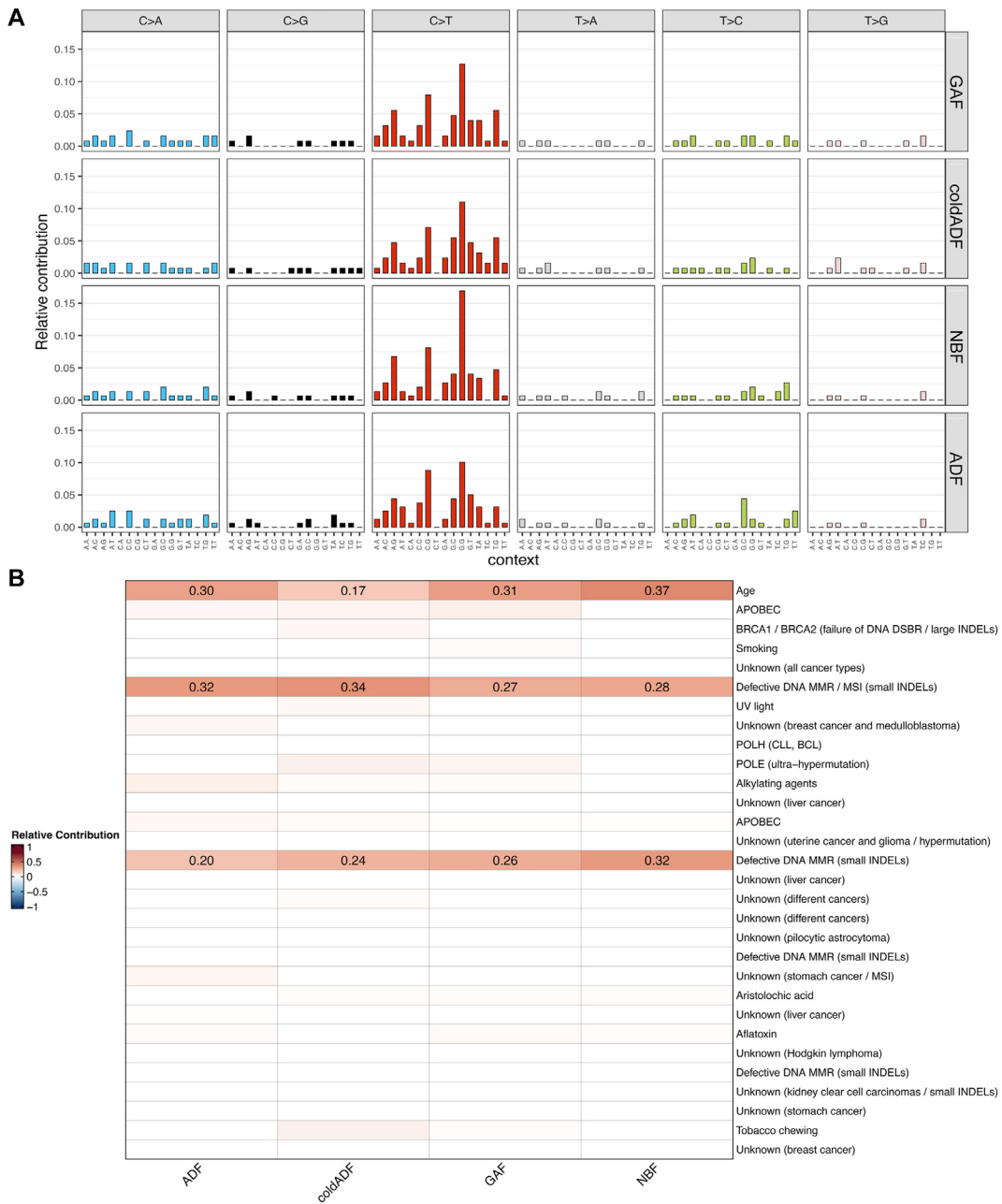
Figure 5.
Mutational signatures derived from the samples. (A) Representation of mutational signatures using the 96-matrix profile based on substitutions identified for the 4 fixation types. The picture reports all the raw substitutions for all samples grouped for the fixation types. (B) Relative contribution of each predicted COSMIC V2 signature for each group. We estimated the mutational signature contribution, comprising all the variants with a VAF >5%. We reported the description of the signatures, sorted up-to-down from signature 1 to 30. ADF, acid-deprived formalin fixation; GAF, glyoxal acid free; NBF, neutral buffered formalin; VAF, variant allele frequency.

and GAF, obtained from acidic glyoxal by the same procedure of resin treatment. Both reagents already provided comparable results with standard FFPE samples when performing ancillary analyses such as IHC and to offer an improvement in DNA preservation.[10,11] In addition, GAF, at variance of formalin, is not cancerogenic or toxic. We previously reported that cold fixation allows better DNA preservation,[14] and therefore, we also tested the combination of acid deprivation and cold formalin fixation.

Based on these premises, we aimed to comprehensively evaluate the impact of different fixation protocols on the performance of data analysis from a CGP approach. We acted at different levels

from preanalytical features to output sequencing results. The DNA yield was equal across different extractions, even when normalizing the total DNA by the size of the lesions. The present study of DNA integrity confirmed and extended our previous report[10] and showed a lower degree of DNA fragmentation for *cold*ADF and ADF samples, which were also the most represented samples in the class with lower fragmentation of the clustering analysis generated from the fragment size distribution data. Similar results were obtained when comparing GAF, an acid-deprived solution of glyoxal, and a buffered solution of the acid commercial glyoxal. These results suggest a clear increase in terms of DNA purity and

structural integrity when fixing tissues with acid deprivation. Of note, the highest level of purity and integrity was obtained with ADF and *cold*ADF, but tissues fixed in acid-deprived glyoxal (GAF) were still superior to NBF in terms of DNA purity and integrity.

The data overall highlight the crucial role played by buffered acids when present in fixatives and support the hypothesis that can be summarized as the "hidden acid theory," where within the microenvironment represented by the cell nucleus, phosphate radicals of nucleic acids can dislodge sodium ions so that formic and other acidic residues are free to affect DNA integrity.[10] We also tested the effect of fixation at low temperature (4 °C) over fixation at room temperature. Confirming a previous study by our group,[14] we observed that the temperature degree is among the multiple factors bound to impact DNA integrity.

We then moved to sequencing performance and data. To objectively assess potential differences across the distinct conditions applied here, we meticulously analyzed several parameters important for library preparation QCs, sequencing QCs, and sequencing results. Overall, significantly longer reads were obtained in libraries from *cold*ADF samples with both the OCAv3 panel and the TSO500 panel. ADF, GAF, and NBF samples followed by the shortest reads demonstrated in NBF samples.

By analyzing OCAv3 panel data, ADF-derived and *cold*ADF-derived libraries showed the lowest level of noise and the highest levels of uniformity, followed by GAF-fixed and NBF-fixed tissues. The TSO500 panel data confirmed the data uniformity. In addition, with this panel, we observed the best performance in terms of total region sequenced for ADF and *cold*ADF samples, whereas NBF samples showed a significantly smaller region sequenced. Along the same lines, NBF samples displayed a significantly lower number of evaluable microsatellite loci compared with all the other fixatives.

Despite formally successful sequencing in all the samples, these QC and sequencing data analyses suggest an increase in terms of the quality of library generation and sequencing outputs from NBF-fixed to GAF-fixed to ADF-fixed and *cold*ADF-fixed samples. One may wonder whether these features affect data reporting and interpretation. Most of the genetic alterations identified were shared by all the samples in each tumoral lesion. Whenever discrepancies were observed across panels and/or samples, we considered "potentially real" a variant identified by both panels. In this respect, 5 genes showed a different status across samples and/or panels. An important observation is that 4 of these discordant results involved samples purified from NBF-fixed tissues, thus suggesting a possible artifactual origin. Although the tissues analyzed here were sampled in parallel from the same region of a given tumoral lesion and we may assume that heterogeneity is highly unlikely, we cannot exclude this alternative explanation for such discordances.

We favor artifacts over biological heterogeneity based on additional data derived from the TSO500 panel. A significantly increased number of SNVs was present in the NBF-fixed lesions, whereas no differences were identified across the other fixation protocols. Finally, when mutational signatures were predicted, signature 1 (aging related but also referred to FFPE artifacts[35]) showed the highest values in NBF samples (37%) and the lowest values in *cold*ADF samples (17%).

One may wish to put into perspective how FFPE-related artifacts are currently dealt with by considering blacklisting specific genomic loci. Nevertheless, blacklisting specific regions is a combination of both sequencing methods and fixation protocols. We may envision that a good practice in molecular diagnostic laboratories in this scenario would be to create a blacklist for each panel first, keeping in mind that the use of ADF is likely to contribute a lesser amount of blacklisting compared with NBF.

In conclusion, fixation is the preliminary, yet central, process in histologic processing leading to the production of paraffin-embedded tissue blocks, the ultimate product constituting the backbone of pathology archives. Different modalities of tissue fixation lead to differential degrees of DNA integrity, which impacts the output of CGP. ADF guarantee the highest DNA preservation overall, thus suggesting the possible implementation of even more complex molecular profiling on tissue samples. Longevity studies assessing the stability of DNA over time on this type of sample are warranted.

Author Contributions

Conceptualization: B.B., G.B., E.B., and C.M. Data curation: E.B., S.E.B., and C.M. Formal analysis: E.B. and S.E.B. Funding acquisition: C.M. and M.C. Investigation: E.B., S.E.B., G.W., A.B., A.C., and A.G. Methodology: E.B., S.E.B., G.B., B.B., A.G., A.N., and M.C. Resources: C.M., A.S., G.B., and B.B. Software: E.B., S.E.B., A.G., A.N., and M.C. Supervision: C.M. and G.B. Visualization: E.B. and S.E.B. Writing—original draft: E.B., G.B., and C.M. Writing—review and editing: all authors. The authors read and approved the final manuscript.

Data Availability

All results are included in the main manuscript and in the additional material. The raw sequencing data related to the clinical samples are not disclosed because they are patient related.

Declaration of Competing Interest

Caterina Marchiò has received personal consultancy fees from Bayer, Roche, Daiichi Sankyo, and AstraZeneca outside the scope of the present work. Paolo Detillo is an employee of ADDAX Biosciences srl. Benedetta Bussolati is cofounder, and Gianni Bussolati serves as CEO of ADDAX Biosciences srl. ADDAX Biosciences srl

developed, patented, and produced both ADF and GAF and provided them for the study. The other authors have no conflicts of interest to declare.

Ethics Approval and Consent to Participate

The Ethics Institutional Review Board responsible for "Biobanking and use of human tissues for experimental studies"—Department of Medical Sciences, University of Turin—approved this study. Specific informed consent was not needed because the parallel samplings relied on leftover material following diagnostic procedures. The study was conducted in accordance with the principles set out in the Declaration of Helsinki.

Supplementary Material

The online version contains supplementary material available at https://doi.org/10.1016/j.labinv.2023.100280

References

1. Mathieson W, Thomas GA. Why formalin-fixed, paraffin-embedded biospecimens must be used in genomic medicine: an evidence-based review and conclusion. *J Histochem Cytochem*. 2020;68(8):543−552. https://doi.org/10.1369/0022155420945050
2. Cucco F, Clipson A, Kennedy H, et al. Mutation screening using formalin-fixed paraffin-embedded tissues: a stratified approach according to DNA quality. *Lab Invest*. 2018;98(8):1084−1092. https://doi.org/10.1038/s41374-018-0066-z
3. Kim S, Park C, Ji Y, et al. Deamination effects in formalin-fixed, paraffin-embedded tissue samples in the era of precision medicine. *J Mol Diagn*. 2017;19(1):137−146. https://doi.org/10.1016/j.jmoldx.2016.09.006
4. Sah S, Chen L, Houghton J, et al. Functional DNA quantification guides accurate next-generation sequencing mutation detection in formalin-fixed, paraffin-embedded tumor biopsies. *Genome Med*. 2013;5(8):77. https://doi.org/10.1186/gm481
5. Hedegaard J, Thorsen K, Lund MK, et al. Next-generation sequencing of RNA and DNA isolated from paired fresh-frozen and formalin-fixed paraffin-embedded samples of human cancer and normal tissue. *PLoS One*. 2014;9(5):e98187. https://doi.org/10.1371/journal.pone.0098187
6. Chen G, Mosier S, Gocke CD, Lin MT, Eshleman JR. Cytosine deamination is a major cause of baseline noise in next-generation sequencing. *Mol Diagn Ther*. 2014;18(5):587−593. https://doi.org/10.1007/s40291-014-0115-2
7. Amemiya K, Hirotsu Y, Oyama T, Omata M. Relationship between formalin reagent and success rate of targeted sequencing analysis using formalin fixed paraffin embedded tissues. *Clin Chim Acta*. 2019;488:129−134. https://doi.org/10.1016/j.cca.2018.11.002
8. Endrullat C, Glokler J, Franke P, Frohme M. Standardization and quality management in next-generation sequencing. *Appl Transl Genom*. 2016;10:2−9. https://doi.org/10.1016/j.atg.2016.06.001
9. Kaneko Y, Kuramochi H, Nakajima G, Inoue Y, Yamamoto M. Degraded DNA may induce discordance of KRAS status between primary colorectal cancer and corresponding liver metastases. *Int J Clin Oncol*. 2014;19(1):113−120. https://doi.org/10.1007/s10147-012-0507-4
10. Berrino E, Annaratone L, Detillo P, et al. Tissue fixation with a formic acid-deprived formalin better preserves DNA integrity over time. *Pathobiology*. 2023;90:155−165. https://doi.org/10.1159/000525523
11. Bussolati G, Annaratone L, Berrino E, et al. Acid-free glyoxal as a substitute of formalin for structural and molecular preservation in tissue samples. *PLoS One*. 2017;12(8):e0182965. https://doi.org/10.1371/journal.pone.0182965
12. Annaratone L, Marchiò C, Sapino A. Tissues under-vacuum to overcome suboptimal preservation. *N Biotechnol*. 2019;52:104−109. https://doi.org/10.1016/j.nbt.2019.05.007
13. Bussolati G, Chiusa L, Cimino A, D'Armento G. Tissue transfer to pathology labs: under vacuum is the safe alternative to formalin. *Virchows Arch*. 2008;452(2):229−231. https://doi.org/10.1007/s00428-007-0529-x
14. Berrino E, Annaratone L, Miglio U, et al. Cold formalin fixation guarantees DNA integrity in formalin fixed paraffin embedded tissues: premises for a

15. Ryska ASA, Landolfi S, Sansano Valero I, et al. Glyoxal acid-free (GAF) histological fixative is a suitable alternative to formalin—results from an open label comparative non-inferiority study. Preprint. Posted online May 28, 2023. medRxiv 20230606. https://doi.org/10.1101/2023.05.24.23290451
16. Sartore-Bianchi A, Pietrantonio F, Lonardi S, et al. Circulating tumor DNA to guide rechallenge with panitumumab in metastatic colorectal cancer: the phase 2 CHRONOS trial. *Nat Med*. 2022;28(8):1612−1618. https://doi.org/10.1038/s41591-022-01886-0
17. Berrino E, Annaratone L, Bellomo SE, et al. Integrative genomic and transcriptomic analyses illuminate the ontology of HER2-low breast carcinomas. *Genome Med*. 2022;14(1):98. https://doi.org/10.1186/s13073-022-01104-z
18. Berrino E, Aquilano MC, Valtorta E, et al. Unique patterns of heterogeneous mismatch repair protein expression in colorectal cancer unveil different degrees of tumor mutational burden and distinct tumor microenvironment features. *Mod Pathol*. 2023;36(2):100012. https://doi.org/10.1016/j.modpat.2022.100012
19. Berrino E, Filippi R, Visintin C, et al. Collision of germline POLE and PMS2 variants in a young patient treated with immune checkpoint inhibitors. *NPJ Precis Oncol*. 2022;6(1):15. https://doi.org/10.1038/s41698-022-00258-8
20. Díaz-Gay M, Vila-Casadesús M, Franch-Expósito S, Hernández-Illán E, Lozano JJ, Castellví-Bel S. Mutational Signatures in Cancer (MuSiCa): a web application to implement mutational signatures analysis in cancer samples. *BMC Bioinformatics*. 2018;19(1):224. https://doi.org/10.1186/s12859-018-2234-y
21. Cereda M, Gambardella G, Benedetti L, et al. Patients with genetically heterogeneous synchronous colorectal cancer carry rare damaging germline mutations in immune-related genes. *Nat Commun*. 2016;7:12072. https://doi.org/10.1038/ncomms12072
22. Alexandrov LB, Nik-Zainal S, Wedge DC, Campbell PJ, Stratton MR. Deciphering signatures of mutational processes operative in human cancer. *Cell Rep*. 2013;3(1):246−259. https://doi.org/10.1016/j.celrep.2012.12.008
23. Annaratone L, De Palma G, Bonizzi G, et al. Basic principles of biobanking: from biological samples to precision medicine for patients. *Virchows Arch*. 2021;479(2):233−246. https://doi.org/10.1007/s00428-021-03151-0
24. AACR Pathology Task Force. Pathology: hub and integrator of modern, multidisciplinary [precision] oncology. *Clin Cancer Res*. 2022;28(2):265−270. https://doi.org/10.1158/1078-0432.CCR-21-1206
25. Fountzilas E, Tsimberidou AM, Vo HH, Kurzrock R. Clinical trial design in the era of precision medicine. *Genome Med*. 2022;14(1):101. https://doi.org/10.1186/s13073-022-01102-1
26. Gouda MA, Nelson BE, Buschhorn L, Wahida A, Subbiah V. Tumor-agnostic precision medicine from the AACR GENIE database: clinical implications. *Clin Cancer Res*. 2023;29:2753−2760. https://doi.org/10.1158/1078-0432.CCR-23-0090
27. Perez EA. Biomarkers and precision medicine in oncology practice and clinical trials. In: Ramirez AG, Trapido EJ, eds. *Advancing the Science of Cancer in Latinos*. 2020:113−123.
28. Yan L, Zhang W. Precision medicine becomes reality-tumor type-agnostic therapy. *Cancer Commun (Lond)*. 2018;38(1):6. https://doi.org/10.1186/s40880-018-0274-3
29. Belloni B, Lambertini C, Nuciforo P, et al. Will PAXgene substitute formalin? A morphological and molecular comparative study using a new fixative system. *J Clin Pathol*. 2013;66(2):124−135. https://doi.org/10.1136/jclinpath-2012-200983
30. Groelz D, Sobin L, Branton P, Compton C, Wyrich R, Rainen L. Non-formalin fixative versus formalin-fixed tissue: a comparison of histology and RNA quality. *Exp Mol Pathol*. 2013;94(1):188−194. https://doi.org/10.1016/j.yexmp.2012.07.002
31. Gundisch S, Schott C, Wolff C, et al. The PAXgene(®) tissue system preserves phosphoproteins in human tissue specimens and enables comprehensive protein biomarker research. *PLoS One*. 2013;8(3):e60638. https://doi.org/10.1371/journal.pone.0060638
32. Kap M, Smedts F, Oosterhuis W, et al. Histological assessment of PAXgene tissue fixation and stabilization reagents. *PLoS One*. 2011;6(11):e27704. https://doi.org/10.1371/journal.pone.0027704
33. Mathieson W, Marcon N, Antunes L, et al. A Critical evaluation of the PAXgene tissue fixation system: morphology, immunohistochemistry, molecular biology, and proteomics. *Am J Clin Pathol*. 2016;146(1):25−40. https://doi.org/10.1093/ajcp/aqw023
34. Southwood M, Krenz T, Cant N, et al. Systematic evaluation of PAXgene® tissue fixation for the histopathological and molecular study of lung cancer. *J Pathol Clin Res*. 2020;6(1):40−54. https://doi.org/10.1002/cjp2.145
35. Guo Q, Lakatos E, Bakir IA, Curtius K, Graham TA, Mustonen V. The mutational signatures of formalin fixation on the human genome. *Nat Commun*. 2022;13(1):4487. https://doi.org/10.1038/s41467-022-32041-5